

**INVESTIGATION ON THE PROPERTIES OF  
NANOSTRUCTURED NICKEL OXIDE LAYER  
FOR HYDROGEN GAS SENSOR**

by

**DAUDA ABUBAKAR**

**Thesis submitted in fulfilment of the requirements  
for the Degree of  
Doctor of Philosophy**

**March 2018**

## ACKNOWLEDGEMENT

Firstly, I will like to thank almighty Allah for granting me this opportunity of finishing my Ph.D. program. I would like to express my great thanks to my supervisor Dr. Naser M. Ahmed, for offering me such opportunity to work on exciting world of nanostructured materials semiconductors and their applications. Altogether, my research work was successfully made under his revealing, patient and brilliant guidance and supervision. His broad information and laborious research attitude have joined me a lot in scientific research. I have been really blessed to have such supervisor who was very much interested about my project, and who always reacted to my inquiries and requests so quickly. I also want to express my great thanks to my co-supervisor, Associate Professor Dr. Shahrom Mahmud, for his support, guidance, patient and invaluable knowledge toward the success of his work. Furthermore, I would like to express my appreciation to our group members of Institute of Nano-Optoelectronics Research and Technology (INOR), School of Physics, Universiti Sains Malaysia (USM) for their great help in the characterization of my samples. My thanks go to Bauchi State University Gadau, Nigeria, for supporting my study financially. Finally, special thanks will be devoted to my entire family due to their continuous prayer, support and encouragement during my study period in Malaysia.

## TABLE OF CONTENT

<b>ACKNOWLEDGEMENT .....</b>	<b>ii</b>
<b>TABLE OF CONTENT.....</b>	<b>iii</b>
<b>LIST OF TABLES.....</b>	<b>viii</b>
<b>LIST OF FIGURES.....</b>	<b>x</b>
<b>LIST OF SYMBOLS .....</b>	<b>xv</b>
<b>LIST OF ABBREVIATIONS .....</b>	<b>xvii</b>
<b>ABSTRAK .....</b>	<b>xix</b>
<b>ABSTRACT .....</b>	<b>xxi</b>
<b>CHAPTER 1: INTRODUCTION .....</b>	<b>1</b>
1.1    Introduction .....	1
1.2    Problem Statements and Motivations .....	3
1.3    Aim and Objectives of the Work .....	5
1.4    Research Originality .....	5
1.5    Outline of Thesis .....	6
<b>CHAPTER 2: BACKGROUND AND LITERATURE REVIEW .....</b>	<b>8</b>
2.1    Introduction .....	8
2.2    Nanostructured Materials .....	8
2.3    Classification of Nanostructures .....	9
2.4    Nanostructured Thin Film Materials .....	11
2.5    Method of Nanostructured Layer Deposition .....	11
2.5.1    Physical Deposition Techniques .....	11
2.5.1(a) Sputtering technique .....	12
2.5.2    Chemical Deposition Techniques .....	13

2.5.2(b) Chemical bath deposition technique .....	13
2.6 Substrate Materials for Film Deposition.....	14
2.7 Nickel Oxide .....	15
2.8 Thermal Oxidation of Nickel .....	18
2.9 Oxidation Mechanism of Nickel .....	18
2.10 Synthesis of Nanostructured NiO Materials .....	19
2.10.1 Reviews on synthesis of Nanostructured NiO layer by Thermal Oxidations of Nickel Metal Thin Film .....	20
2.10.2 Reviews on synthesis of Nanostructured NiO layer by Chemical Bath Deposition .....	23
2.11 Gas Sensor.....	27
2.12 Metal Oxide Gas Sensors.....	28
2.12.1 Chemiresistive Gas Sensors.....	29
2.12.2 Metal Oxide based Gas Sensing principle .....	31
2.13 Factors Influencing Sensing Performance .....	34
2.14 Basic Characteristics of Metal Oxide Gas Sensing .....	35
2.15 Electrodes for Metal Oxide Gas Sensors .....	37
2.15.1 Electrode Configuration for Metal Oxide Gas Sensors.....	38
2.15.2 The Two-Electrode Configuration.....	38
2.15.3 The Interdigitated Electrodes.....	39
2.15.4 Electrode Materials for Semiconductor Gas Sensors .....	40
2.16 Interfacial of Electrode-Semiconductor Contact .....	40
2.16.1 Ohmic Contact using Work Function .....	42
2.16.2 Ohmic Contact using Tunnelling .....	44
2.17 Hydrogen Gas Sensors .....	45

2.17.1	Hydrogen Sensing Mechanism on Properties of Nanostructured NiO layer .....	47
2.17.2	Reviews on Hydrogen Gas Sensors using Nanostructured Nickel Oxide.....	49
<b>CHAPTER 3: METHODOLOGY AND INSTRUMENTATION .....</b>		<b>54</b>
3.1	Introduction .....	54
3.2	Substrate Cleaning and Seed Layer Deposition .....	56
3.3	Synthesis of Nanostructured NiO Layer using Chemical Bath Deposition of Ni(OH) <sub>2</sub> Layer .....	57
3.3.1	Sample Preparation .....	57
3.3.2	Mechanism .....	58
3.4	Synthesis of Nanostructured NiO Layer by Thermal Oxidation of Metallic Ni Layer. ....	61
3.4.1	Sample Preparation .....	61
3.4.2	Procedure of Nickel Oxidation .....	62
3.5	Characterization Techniques .....	63
3.5.1	X –Ray Diffraction .....	64
3.5.2	Field Emission Scanning Electron Microscopy .....	67
3.5.3	Energy Dispersive X-Ray Spectroscopy .....	68
3.5.4	Atomic Force Microscopy .....	70
3.5.5	Ultra Violet-Visible Spectroscopy .....	71
3.5.6	Annealing Compact Tube Furnace .....	74
3.6	Device Fabrication of NiO Nanomaterials for Hydrogen Gas Sensor.....	75

3.6.1	Fabrication Gas sensor testing system of Nanostructured NiO Layer .....	75
-------	---	----

**CHAPTER 4: NANOSTRUCTURED NiO LAYER BY CHEMICAL BATH**

**DEPOSITION FOR HYDROGEN GAS SENSOR**

	<b>APPLICATION .....</b>	<b>79</b>
4.1	Introduction .....	79
4.2	Effect of Molar Concentration of NiSO <sub>4</sub> •6H <sub>2</sub> O on the Structural Properties .....	79
4.3	Effect of Seed Layer on the Structural Property of NiO Layer .....	81
4.4	Effect of Solution Mixture with and without Potassium Chloride on the Morphological Properties .....	82
4.5	Effect of Annealing Temperature on the Morphological Properties .....	83
4.6	Effect of Annealing Temperature on the Structural Properties .....	86
4.7	Effect of Annealing Temperature on the Energy Band Gap .....	88
4.8	Performance of Hydrogen Gas Sensor Based on Chemical Bath Deposition of NiO Growth.....	90

**CHAPTER 5: NANOSTRUCTURED NiO LAYER BY THERMAL**

**OXIDATION FOR HYDROGEN GAS SENSIN**

	<b>APPLICATION .....</b>	<b>99</b>
5.1	Introduction .....	99
5.2	Effect of Film Thickness and Annealing Time on the Structural Properties .....	99
5.3	Effect of Substrate Layer on the Structural and Morphological Properties .....	101

5.4	Effect of Annealing Temperature on the Structural, Morphological and Optical Properties.....	102
5.5	Performance of Hydrogen Gas Sensor Based on Thermal Oxidation of NiO Growth.....	107
<b>CHAPTER 6: CONCLUSIONS AND FUTURE WORK .....</b>		<b>115</b>
6.1	Conclusions .....	115
6.2	Future Works .....	117
<b>REFERENCE .....</b>		<b>119</b>
<b>LIST OF PUBLICATIONS</b>		

## LIST OF TABLES

		<b>Page</b>
Table 2.1	Fundamental properties of NiO	18
Table 2.2	The survey of NiO synthesized from literature by thermal dry oxidation of Nickel	22
Table 2.3	The survey of NiO synthesized from literature by CBD method	25
Table 2.4	The lower explosive limit (LEL) and ignition temperature of some common explosive gases	28
Table 2.5	Difference in gas response change with different semiconducting sensing element	34
Table 2.6	The survey of NiO layer membrane for H <sub>2</sub> gas sensor	52
Table 3.1	Variable parameters used for the growth of NiO layer	57
Table 3.2	Parameter used in RF sputtering of Nickel thin film	61
Table 3.3	NiO samples conditions and Hydrogen gas sensing/testing parameters	78
Table 4.1	Atomic and weight percent of the as-grown and annealed sample obtained from EDS spectrum and corresponding flakes width and layer thickness	85
Table 4.2	Roughness of root mean square of as-grown and annealing samples, deduce from AFM analysis	86
Table 4.3	Variable parameters used in crystal size calculation	88
Table 4.4	Values of variable voltage for hydrogen gas response	91
Table 4.5	Power consumption at different operating temperature	96
Table 5.1	Crystal size obtained from XRD analysis base on FWHM and 2 $\theta$ for oxidation samples	104

Table 5.2	Nanostructured NiO layer width dimension, thickness and oxidation at different annealing temperature	105
Table 5.3	Roughness of root mean square obtained from AFM for oxidation samples	106
Table 5.4	Values of variable voltage for hydrogen gas response	108
Table 5.5	Response and recovery time at different operating temperature	112
Table 5.6	Power consumption at different operating temperature	113

## LIST OF FIGURES

		<b>Page</b>
Figure 2.1	Classification of nanostructured materials based on 0D, 1D, 2D, and 3D.	10
Figure 2.2	Simple sketch of sputtering system.	12
Figure 2.3	Simple setup for chemical bath deposition.	14
Figure 2.4	Unit cell of NiO.	16
Figure 2.5	Excess "O" in NiO leads to cation vacancies and makes it a p-type semiconductor.	17
Figure 2.6	Grain boundary showing the potential high with and without reducing gas	32
Figure 2.7	Representation of semiconductor metal oxide gas sensors.	33
Figure 2.8	Chemiresistive gas sensor response-curve.	36
Figure 2.9	The interdigitated electrodes used in gas sensor	39
Figure 2.10	Band structure of metal and n- and p-type semiconductor with respective work functions	42
Figure 2.11	Metal to n-type semiconductor Junction with (a) work function metal greater than n-type and bands bend up forming barrier and (b) work function of metal less than n-type and bands bend down forming no barrier.	43
Figure 2.12	Metal to p-type semiconductor junction with (a) work function of metal greater than p-type and bands bend up forming no barrier and (b) metal work function less than p-type and bands bend down forming barrier.	44

Figure 2.13	Metal to semiconductor junction showing the sharper bend due to (a) n <sup>+</sup> type region and (b) p <sup>+</sup> type semiconductors region causing thin barrier that allows quantum tunnelling of electron.	45
Figure 2.14	The increase and decrease of the depletion layer of NiO nanoflakes sensor	47
Figure 3.1	Flowchart for hydrogen gas sensor fabrication based on Nanostructured NiO layer	55
Figure 3.2	Chemical bath deposition of Ni(OH) <sub>2</sub> thin film	58
Figure 3.3	Ionic structure of tetrachloronickelate (II) complex ion	59
Figure 3.4	Ionic structure of hexammine complex ion	59
Figure 3.5	RF sputtering deposition of Ni metal thin film	61
Figure 3.6	X-ray reflections from a crystal.	64
Figure 3.7	Schematics diagram of X-ray diffractometer.	65
Figure 3.8	High Resolution X-Ray Diffractometer System (Model PANalytical X'Pert PRO MRD PW3040) of NOR Lab	66
Figure 3.9	Schematics diagram of field emission scanning electron microscopy	67
Figure 3.10	Field Emission Scanning Electron Microscope (FESEM) & EDX/EBSD Detector (Model FEI Nova NanoSEM 450) of INOR lab.	69
Figure 3.11	Sketch of Atomic Force Microscope and AFM (Model: Dimension 71 EDGE, BRUKER) of INOR Lab.	71
Figure 3.12	Schematic diagram of an UV-visible spectrophotometer and UV-Visible Spectrophotometer (Model Cary 5000 UV-VIS-NIR) of INOR Lab.	72
Figure 3.13	Compact tube furnace of INOR Lab.	74

Figure 3.14	Pt electrode deposited on synthesized NiO layer on ITO/glass substrate	75
Figure 3.15	Schematic diagram of hydrogen gas sensing setup system	77
Figure 4.1	Solution prepared at (a) 0.2, (b) 0.5 and (c) 1.0 molarities of $\text{NiSO}_4 \cdot 6\text{H}_2\text{O}$ at 200 °C annealing temperature for 90 min	80
Figure 4.2	AFM analysis for ITO/Glass substrate	81
Figure 4.3	XDR analytical result of NiO growth on glass and ITO/glass substrates treated at 200 °C for 90 min	82
Figure 4.4	FESEM analytical result on as-grown $\text{Ni}(\text{OH})_2$ grown (a) with KCl (inset of nanoflakes dimension) and (b) without KCl in the solution	83
Figure 4.5	FESEM and EDX image of NiO nanoflakes with inset of cross-section layer thickness for (a) as-grown, (b) 200, (c) 300 and (d) 400 °C samples treatment.	84
Figure 4.6	Typical AFM surface images of NiO/ $\text{Ni}(\text{OH})_2$ for (a) as grown (b) 200 (c) 300 and (d) 400 °C layer samples	86
Figure 4.7	XRD pattern of the NiO/ $\text{Ni}(\text{OH})_2$ nanoflakes for (a) as-grown, (b) 200, (c) 300 and (d) 400 °C annealing temperature.	88
Figure 4.8	Plot of absorption coefficient against wavelength with an inset of the corresponding energy band gap of NiO at (a) 200, (b) 300 and (c) 400 °C annealing temperatures	89
Figure 4.9	I-V characteristic for Pt-NiO contact for CBD grown sample at 300 °C	91
Figure 4.10	Change in resistance of NiO nanoflakes at different concentrations of hydrogen gas introduction and banishment for (a) RT, (b) 50, (c) 75, (d) 100, (e) 125 and (f) 175 °C operating temperatures.	93

Figure 4.11	Hydrogen gas response at different operating temperature at 1000 ppm	94
Figure 4.12	The response cycle at (a) (a) RT, (b) 50, (c) 75, (d) 100, (e) 125 and (f) 175 °C different operating temperature	95
Figure 4.13	Plot of power consumption against operating temperature	96
Figure 5.1	XRD analysis on different duration of annealing	100
Figure 5.2	XRD analysis on different thickness for 2 hours	101
Figure 5.3	(a) XRD pattern of NiO on ITO/Glass and glass, and FESEM image of NiO on (b) ITO/Glass and (c) glass substrate	102
Figure 5.4	XRD results on dry oxidation of Nickel thin film at different annealing temperature	104
Figure 5.5	FESEM and EDX image of nanostructure NiO with inset of cross-section layer thickness at (a) 400, (b) 450, (c) 500, (d) 550 and (e) 600 °C annealing temperature	105
Figure 5.6	Typical 2D AFM surface images of NiO layer at (a) 400, (b) 450, (c) 500, (d) 550 and (e) 600 °C annealing temperature	106
Figure 5.7	Plot of absorption coefficient against wavelength with an inset of the corresponding energy band gap of NiO at (a) 400, (b) 450, (c) 500, (d) 550 and (e) 600 °C annealing temperatures	107
Figure 5.8	I-V characteristic for Pt-NiO contact for thermal oxidation grown sample at 550 °C	108
Figure 5.9	Change in resistance of nanostructured NiO layer at different concentrations of hydrogen gas introduction and banishment for (a) RT, (b) 50, (c) 100 and (d) 150 °C operating temperatures	109
Figure 5.10	Hydrogen gas response at different operating temperature for 1000 ppm	110

Figure 5.11	The response cycle at (a) RT, (b) 50, (c) 100 and (d) 150 °C operating temperature for 1000 ppm	111
Figure 5.12	The response and recovery time obtained at different operating temperature	112
Figure 5.13	The power consumption at different operating temperature	113

## LIST OF SYMBOLS

$\alpha$	absorption coefficient
$\alpha_0$	parameter of band tailing
$\beta$	full width at half maxima of the peak
$\theta$	diffraction angle
$\mu$	mobility
$\nu$	incident photons frequency
$\rho$	resistivity
$\phi_m$	metal work function
$\phi_{p-sc}$	p type semiconductor work function
$A$	refractive index coefficient
$a$	lattice cell parameters
$\text{\AA}$	angstrom
$C_1$	hydrogen gas cylinder concentration
$D$	crystals size
$d$	interplanar spacing
$E_g$	optical energy band gap
eV	electron volt
$F_H$	flow of hydrogen gas
$F_{H+N}$	flow of hydrogen gas diluted with nitrogen gas
$h$	Planck's constant
$H_2$	hydrogen gas
h $\nu$	photon energy
$I$	transmitted intensities
$I_o$	incident intensities

I-V	current voltage characteristics
k	constant
$l$	wavelength
M	molarity
n	index constant
$n$	order of diffraction
$\text{Ni}^{2+}$	nickel ions
$\text{N}_2$	nitrogen gas
$\text{O}^{2-}$	oxygen ions
PC	personal computer
pH	potential of hydrogen
$p_H$	hole concentration
$q$	diffraction angle
R	roughness
$R$	electrical resistance
$R_{air}$	measured resistance response with air presence
$R_H$	average Hall coefficient
$R_{gas}$	measured resistance response with target gas
$S_B$	responses of the sensor to B gas
$S_A$	responses of the sensor to Hydrogen gas
T	temperature
$t$	thickness
$T$	transmittance
$V$	applied bias voltage

## LIST OF ABBREVIATION

0-D	zero dimensional
1-D	one dimensional
2-D	two dimensional
3-D	three dimensional
AC	alternating current
AFM	atomic force microscope
CB	catalytic bead
CBD	chemical bath deposition
CuO	copper oxide
DC	direct current
EDX	energy dispersion X-ray
FESEM	field emission scanning electron microscopy
FTIR	fourier transform infrared spectroscopy microscopy,
FWHM	full width at half maxima
GC	gas chromatograph
ICDD	International Centre for Diffraction Data
ITO	indium tin oxide
IVHM	Integrated Vehicle Health Monitoring
JCPDS	Joint Committee Powder Diffraction Standards
KCl	potassium chloride
LEL	lower explosive limit
MS	mass spectrometry
NASA	National Aeronautics and Space Administration
NH <sub>3</sub>	ammonia

NFPA	National Fire Protection Association
NiO	nickel oxide
Ni(OH) <sub>2</sub>	nickel hydroxide
NMR	nuclear magnetic resonance spectroscopy
PLD	pulse laser deposition method
PMMA	polymer of methyl methacrylate
ppm	parts per million
PS	polystyrene
RF	radio frequency
RT	room temperature
SIMS	secondary ion mass spectrometry
SnO <sub>2</sub>	tin oxide
TEM	transmission electron microscopy
TFTs	thin-film-transistor
UV-Vis	ultra violet-visible spectroscopy
XPS	X-ray photoelectron spectroscopy
XRD	X-ray diffraction
ZnO	zinc oxide

# **KAJIAN KE ATAS SIFAT STRUKTUR NANO LAPISAN NIKEL OKSIDA SEBAGAI PENGESAN GAS HYDROGEN**

## **ABSTRAK**

Dalam kajian ini, lapisan struktur nano NiO disintesis menggunakan enapan rendaman kimia (CBD) dan pengoksidaan terma untuk sensor gas H<sub>2</sub> berprestasi tinggi. Proses sintesis lapisan struktur nano NiO dikawal berdasarkan beberapa penambahan parameter yang berbeza-beza dalam setiap kaedah pemendapan. Setiap struktur, morfologi dan sifat optik lapisan struktur nano NiO dikaji menggunakan XRD, FESEM, EDX dan Spektrometer UV-Vis. Saiz kristal, kekasaran permukaan, rongga permukaan, ketebalan lapisan dan sifat kekristalan adalah faktor yang mempunyai mempengaruhi yang besar bagi meningkatkan kejayaan untuk mengesan gas H<sub>2</sub>. Kurang penekanan terhadap faktor-faktor ini merupakan sebab utama mengapa kebanyakan laporan kajian tentang NiO berkait sensor gas H<sub>2</sub> menunjukkan pencapaian pengesanan yang rendah. Tumpuan dalam kajian ini bertujuan untuk meningkatkan pencapaian pengesanan gas H<sub>2</sub> terhadap faktor-faktor tersebut. Sampel lapisan NiO yang berkembang pada 300 ° C (CBD) dan 550 ° C (pengoksidaan terma) ke atas ITO / substrat kaca menunjukkan keputusan yang baik bagi meningkatkan pencapaian pengesanan gas H<sub>2</sub> dan digunakan sebagai pengesanan membran untuk sensor gas H<sub>2</sub>. Ciri-ciri pengesanan lapisan nano struktur NiO diteliti berdasarkan kepekatan gas H<sub>2</sub> dan suhu operasinya. Didapati rangsangan gas H<sub>2</sub> (sensiviti) menurun pada peningkatan suhu operasi kerana faktor kelembapan yang tinggi (~ 80 %) pada suhu yang rendah dan (25 °C) pada peningkatan rintangan. Kelembapan suhu menurun akibat penurunan rintangan. Sampel asas CBD menunjukkan tindak balas gas H<sub>2</sub> yang lebih tinggi (iaitu 50.44) di RT (25 °C) berbanding sampel asas pengoksidaan termal (iaitu 3.12) kerana saiz

kristal yang lebih kecil (iaitu 19.84 nm), kekasaran yang lebih banyak (iaitu 75.2 nm) saiz (iaitu 300 nm) dan ketebalan lapisan yang dipertingkatkan (iaitu 683.7 nm). Selain itu, penggunaan kuasa pada RT (25 °) ke atas sampel asas CBD adalah lebih rendah (iaitu 0.13 mW) daripada sampel asas pengoksidaan terma (iaitu 2.7 mW) disebabkan tindak balas sampel CBD pada rintangan yang lebih tinggi (iaitu 1975  $\Omega$ ). Tindak balas dan masa pemulihan tidak dapat ditentukan untuk sampel CBD disebabkan oleh tidak ada tahap tepu gas H<sub>2</sub> pada setiap selang masa 5 minit. Walau bagaimanapun, sampel asas pengoksidaan terma mempunyai tahap tepu yang baik terhadap tindak balas gas H<sub>2</sub>. Oleh kerana lapisan NiO tidak digunakan secara komersial sebagai sensor gas H<sub>2</sub> dan kebanyakan laporan mengenai kajian NiO sensor gas H<sub>2</sub> menunjukkan tindak balas yang lebih rendah (iaitu > 3.0) dengan tindak balas dan masa pemulihan yang perlahan (iaitu < 47 s) berbanding dengan penemuan dalam kajian ini. Oleh itu, penemuan ini berkemungkinan bernilai untuk merekabentuk peranti bagi sensor gas H<sub>2</sub> bercapaian tinggi menggunakan struktur nano NiO.

# INVESTIGATION ON THE PROPERTIES OF NANOSTRUCTURED NICKEL OXIDE LAYER FOR HYDROGEN GAS SENSOR

## ABSTRACT

In this work, nanostructured NiO layers were synthesized using chemical bath deposition (CBD) and thermal oxidation methods for high performance of H<sub>2</sub> gas sensor. The synthesis of nanostructured NiO layer was controlled base on several growth parameters which were varied in each deposition methods. The structural, morphological, and optical properties of nanostructured NiO layer were studied using XRD, FESEM, EDX and UV-Vis spectrometer. The crystal size, surface roughness, porous surface, layer thickness, and crystallinity are factors that have great influence in enhancing the H<sub>2</sub> gas sensing performance. These factors are the main reason why most report on NiO for H<sub>2</sub> gas sensor shows poor sensing performance. Thus, the focus of this report is to enhance the H<sub>2</sub> gas sensing performance base on these factors. The nanostructured NiO layer samples that were grown at 300 °C (CBD) and 550 °C (thermal oxidation) on ITO/glass substrates show good results needed for improving H<sub>2</sub> gas sensing performance and used as the sensing membranes for H<sub>2</sub> gas sensor. The H<sub>2</sub> gas sensing properties of nanostructured NiO layer were studied based on the H<sub>2</sub> gas concentration and operating temperature. It was observed that the H<sub>2</sub> gas response (sensitivity) decreases with increase in operating temperature due to high humidity (i.e. ~ 80 %) at low temperatures (i.e. 25 °C) that increases the resistance. The effect of humidity decreases with temperature resulting in decreasing the resistance. The CBD base sample shows higher H<sub>2</sub> gas response (i.e. 50.44) at RT (25 °C) than thermal oxidation base sample (i.e. 3.12) due to its smaller crystal size (i.e. 19.84 nm), higher roughness (i.e. 75.2 nm), higher pore size (i.e. 300 nm) and higher layer thickness

(i.e. 683.7 nm). Likewise, the power consumption at RT (25 °) of the CBD sample is lower (i.e. 0.13 mW) than thermal oxidation sample (i.e. 2.7 mW) due to the response of the CBD sample at higher resistance (i.e. 1975 Ω). The response and recovery time were undetermined for CBD sample due to the absence of saturation peak of H<sub>2</sub> gas at 5 min time interval. But the thermal oxidation base sample appears to have good saturation peak of the H<sub>2</sub> gas response. The response and recovery time decreases with temperature due to higher adsorption/desorption processes at higher temperature (i.e. < 25 °) with the fastest time of 6.1 and 0.5 s respectively at 150 °C. Since NiO layer has not been used as a commercial H<sub>2</sub> gas sensor and most report on NiO test for H<sub>2</sub> gas sensor shows lower response (i.e. > 3.0) with slow response and recovery time (i.e. < 47 s) as compared to this report. Therefore, this finding may be valuable to design a device for the H<sub>2</sub> gas sensor with high performance using nanostructured NiO layer.

# CHAPTER 1

## INTRODUCTION

### 1.1 Introduction

Nanostructured metal oxide materials have been extremely used for different application in science and technology and to get new type of functional materials with great properties and applications. Nickel oxide (NiO) is usually considered, being a model of p-type semi conducting material as it belongs to transition metal oxide semiconductor. It has cubic or rhombohedral structure, but cubic structure is the most commonly adopted structure [1]. Nanostructured NiO have attracted great attention because of its great electrochemical effect, good chemical durability and stability, low cost device application [2] and wide energy band gap (3.6 - 4.0 eV) [3]. These properties make it ideal material for numerous device applications in nanoelectronics fields. These include electrochemical charging/discharging mechanism [4,5], as counter electrode in smart windows [6], as active material in biosensors and chemical sensors [7], light shutter and variable reflectance mirrors in optoelectronic devices [8], solar cell device [9] etc.

To date, various types of nanostructured NiO have been grown. These include nanoparticles [10], nanoflakes [11], nanowires [12], nanotubes [13], and nanorods [14] etc. Several of chemical and physical techniques, such as chemical bath deposition (CBD) [15], Spray pyrolysis [16], RF and DC Sputtering [17,18], electrochemical deposition [19], thermal oxidation [20], hydrothermal method [21], sol-gel method [22], pulse laser deposition method (PLD) [23] etc., has been used to enhance the functionality of nanostructured layer. Among these preparation techniques, the thermal oxidation of RF sputtered Ni metal and chemical bath

depositions were employed in this work, due to its convenient for high porous surface layer deposition with wide surface area.

Hydrogen is colorless, tasteless, and odorless gas which cannot be detected by human sense and it requested highly sensitive device to detect its presence. The wide flammable range and low ignition energy makes hydrogen easy explosive and inflammable. Hydrogen is used in biomedical, metal smelting, rocket fuels, glassmaking, petroleum extraction, semiconductor processing, chemical industry, environmental protection, etc., due to its strong reducing properties [24]. The traditional hydrogen detectors such as gas mass spectrometers, chromatographs and ionization gas pressure sensors are limited by their high temperature, expensive cost, slow response and large size. Hydrogen gas sensors of lower production cost, smaller size, faster response time, lower operation temperature and low power consumption are needed for in-situ and portable monitoring. The rapid development of the hydrogen economy has promoted research on new types of hydrogen gas sensors with more rapid and accurate hydrogen sensing, at or near room temperature operation [25,26].

Nanostructured metal oxide materials provide special properties than its bulk materials and these properties results to a great enhancement on the sensors response. Changing the shape and size of nanostructured materials is a commonly used strategy to optimize their performance due to their nanostructure properties dependent. Nanocomposite materials such as nanoflakes, nanosheet, etc. serve as the backbone pillars for functional nanostructured devices and provide perfect electron and hole efficient transport [27]. Comparing the bulk materials for gas sensors device applications, it shows greater gas sensing enhancement and response for outstanding requirement of gas sensing properties [28].

Porous nanostructured NiO with chemical and physical properties of high stability was considered as one of the most promising semiconductor metal oxide materials for biosensor and chemical sensor applications, owing to its good optical, structural, and morphological properties. Nanoporous NiO layer of nanometer pores size have attracted attention of various researchers in the field of nanomaterials due to its larger surface area [29]. It turns out to have great performance than the bulk structured, particularly in electrochemical applications [30]. Moreover, nanoporous NiO layer give a high surface area- to-volume ratio, which is an important factor for great performance of sensing device [31]. NiO are mostly not used in gas sensor device due its poor performance as shown Table 2.6. Several metal oxide used as materials for hydrogen sensing are *n*-type semiconductors [32], while NiO with *p*-type conduction can also be considered for hydrogen sensing. Hence, the work is dedicated to see the possible application of nanostructured NiO layer for hydrogen gas (H<sub>2</sub>) gas sensor using two dissimilar deposition techniques.

## 1.2 Problem Statements and Motivation

The hydrogen gas is used in many sectors. Been the lightest elements with smallest size of molecule, its leakage in process of production, storage and usage, is possible and might result to some dangers, due to low minimum ignition energy (0.017 mJ), high heat of combustion (142 kJ/g) and wide flammable range (4–75%) [24,25]. Therefore, rapid and accurate hydrogen detection is necessary.

For the past decade, nanostructured metal oxide has been extremely investigated on its usage for different applications, such as gas sensing. The metal oxides semiconductors of Tungsten oxide, Zinc oxide, Tin oxide, etc. [32-34] have been studied as gas sensing material more deeply. Though, these materials may perform better, but their sources may not be available in some part of the world,

which will result in higher production cost. Recently, the discovery made by Titan Nickel project in the northern Nigeria, yielded some interesting results of high-grade native nickel which was believed to have never been documented before anywhere in the world [35]. Therefore, this urge the need to employ the use of NiO synthesis using thermal oxidation of nickel metal for H<sub>2</sub> gas sensor to explore more option.

The porous NiO layer may provide a higher surface area that is considered to be an essential parameter in operations of higher sensing performance for hydrogen gas sensing [30,36,37]. But less focus has been given on NiO nanoflakes with higher porous surface layer for hydrogen gas sensor application.

The fabrication of hydrogen gas sensor devices are commonly made on glass, alumina, quartz or silicon substrates [38-44], But the brittleness of silicon and high cost of alumina, quartz and silicon are some major drawbacks for their application in gas sensor device fabrication as compared to glass.

Most reports published on the use of nanostructured NiO layer for hydrogen gas sensor shows poor response at low temperature such as lower sensitivity, higher detection limit, higher operating temperature, slower response and recovery time. The poor response were associated to lower surface roughness [45,46], larger crystal size [47,48], thinner sensing layer [45,49] and lesser porous morphological surface layer [50].

The present commercial gas sensors of hydrogen gas required elevated substrate temperatures resulting in additional heating system, which greatly increases power consumption and sensor size. Hydrogen gas sensor that operates at or near room temperature may have extreme ability to operate in inflammable environments safely and requires low power consumption with smaller sensor size [51,52].

### **1.3 Aim and Objectives of the Work**

The principal aim of this thesis is to prepare Nickel oxide layer by physical and chemical deposition technique for hydrogen sensors device applications. The objective of the study is:

- To synthesize nanostructured NiO layer with good quality using chemical bath deposition of Ni(OH)<sub>2</sub> and thermal oxidation of Nickel metal deposited using RF sputtering method based on different annealing temperatures for higher response of H<sub>2</sub> sensor.
- To improve the nanostructured NiO layer using ITO/glass substrate for higher H<sub>2</sub> gas response performance
- To investigate the structural and morphological properties of synthesized NiO layer based on the factors (surface roughness, surface area, crystal size, thickness and surface morphology) responsible for higher performance of H<sub>2</sub> gas sensor
- To fabricate and evaluate H<sub>2</sub> gas sensor based on selected nanostructured NiO layer with factors responsible for high sensing performance at or near room temperature.

### **1.4 Research Originality**

This research provides the following originality to overcome the problems stated in Section 1.2

- 1- Selection of good deposition properties of Ni layer (such as method, substrate temperature, operation power, Ni thickness) for thermal oxidation of nickel layer that can show more enhancement of NiO layer quality after annealing.

- 2- Selection of good deposition properties of Ni(OH)<sub>2</sub> (such as precursor mixture, molarity and volume; deposition temperature and duration) for CBD that can show more enhancement of NiO layer quality after annealing.
- 3- Deposition of nanostructured NiO layer on ITO seed layer (with selected thickness) that can enhanced the nanostructured NiO layer
- 4- Fabrication of H<sub>2</sub> gas sensor base on selected nanoflakes and nanoporous NiO layers synthesized base on CBD and thermal oxidation respectively, that can provide higher detection ability at different concentration and lower operating temperature.

## 1.5 Outline of Thesis

Chapter 1 gives the research problems, research objectives, and research originality that associated to this project.

Chapter 2 discussed some background and literature review on the properties of nanostructured metal oxide material, their different growth and fabrication (mainly nanostructured NiO layer). Its application to gas sensor device (particularly H<sub>2</sub> gas sensor). Also, it provides the principles of growth mechanisms as well as fundamental bases of H<sub>2</sub> gas sensing characteristics and performance.

Chapter 3 provides the methodology and instrumentation that have been employed in the nanostructured NiO preparation and for device sensing applications.

Chapter 4 discussed the production mechanism and characterization results of NiO layer, deposition via chemical bath method under different growth conditions as well as its hydrogen gas sensing properties which depend on the different operating temperature and gas concentration.

Chapter 5 present the growth mechanism and characterization results of NiO, deposition via thermal oxidation approach in a furnace tube with different growth

parameters. The hydrogen gas sensing properties were discussed based on the characterization of hydrogen gas under wide concentrations ranging at different operating temperature.

Chapter 6, highlight some important remarks on the obtained results and future research studies.

## CHAPTER 2

### BACKGROUND AND LITERATURE REVIEW

#### 2.1 Introduction

This chapter contains the background and literature review of the research project, which deals with the basic knowledge required for understanding the synthesis and fabrication properties of nanostructured NiO thin film material. The brief explanation of the fundamental principles and formation mechanisms of nanomaterial via thermal oxidation, and chemical bath deposition are addressed and related it to literature reviews on material productions. The theoretical background, sensing mechanism and properties of gas sensor (basically hydrogen gas sensor) are given in this chapter with the discussion on related literature review for hydrogen gas sensing application of nanostructured NiO materials.

#### 2.2 Nanostructured Materials

Nanostructured materials had its origin from big-bang, although the deliberate and controlled nanostructured materials by human started at recent time. The evolutionary structure of the initial meteorites assumed that atoms were first merged into nanostructured scale masses, which then under the gravitational action combined into bigger masses. Several illustrations of natural nanostructured material can be obtained in biological systems [53].

Nanostructured materials have volume size that is transitional among microscopic and molecular structures. The physical and chemical properties of nanostructured materials are separated from those of microscopic and bulk structural materials. The synthesis methods of nanostructured materials provide us with a way of nanometric scale arrangement. One nanometer size is about similar to the

combined size of four atoms, that is about 50,000 smaller times than diameter of normal human hair [54]

The most common definition for nanostructured materials scale measurement were taken to be below 100 nm. Nanostructured materials attracted great attention in science due to its potential application such as biomedicine, catalysis, electronics, cosmetics, high-performance composites, environmental analysis and remediation, electronics, magnetic recording, lasers, structural materials, sensors, imaging technology, etc [55,56]. These have encouraged the speedy development of nanoscience. For the past years interesting development has been achieved by science base research community in depositing, synthesizing, characterizing and processing nanostructured materials.

Nanostructured materials of metals such as Ni, Al, Pt, etc., and metal oxides such as TiO<sub>2</sub>, NiO, ZnO etc., have demonstrated an enhanced properties of catalytic action behavior because of their high surface to volume ratio area. This enhancement plays great roles in several scientific areas such as purification of water, chemical industry, etc. Gas sensors device based on transition metal oxides have several preferred advantages over the gas sensors of conventional type. The advantages are lower operating temperature, higher gas response etc. [57]. The logical investigation of the nanostructured materials properties has brought the most expected solution for the search of materials with perfect properties in the field of science and technology.

### **2.3 Classification of Nanostructures**

Nanostructured materials are diversely classified into several types. Classifying nanostructured materials based on their dimensional properties is the most common style classification. As shown in Figure 2.1, nanostructured materials

can be labelled as zero- (0D), one- (1-D), two- (2-D) and three-dimensional (3-D) [53].

**0-D**

**All dimensions (x, y, z) at nanometric scale**

**Example: Nanoparticles or Nanospheres**

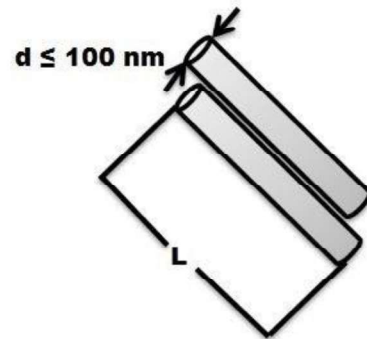


**1-D**

**Two dimensions (x, y) at nanometric scale**

**One dimension (L) is not**

**Example: Nanorods, Nanotubes**

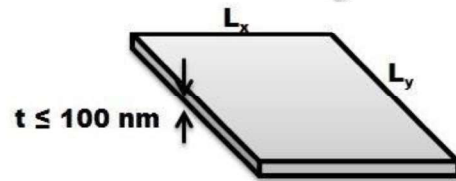


**2-D**

**One dimension (t) at nanometric scale**

**Two dimension (L<sub>x</sub>, L<sub>y</sub>) are not**

**Example: Thin Nanofilms, Nanosheet, Nanoflakes**



**3-D**

**All of dimension (L<sub>x</sub>, L<sub>y</sub>, L<sub>z</sub>) are not at nanometric scale**

**Example: Nanocrystals, Nanocomposite materials**

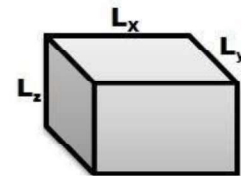


Figure 2.1: Classification of nanostructured materials based on 0D, 1D, 2D, and 3D [58]

The 0-D nanostructures are in the range of nanometric size (examples are nanopowders, nanospheres, nanoparticles and nanoclusters). The 1-D nanostructures possess a nanometric dimensional size which is outside the range with a rod like shapes, and it comprise of nanowires, nanotubes, nanoneedles and nanorods. The 2-D nanostructures possess two nanometric dimensional size which were outside the range, it consists of thin nanofilms, nanocoating, nanolayers, nanosheets nanowalls, and nanoflakes. The 3-D nanostructures have three nanometric size dimensions which were outside the 100 nm range with several distributions of nanocrystallites, nanolayers and nanoparticles and also groups of nanotubes, nanorods and nanowires [27].

## **2.4 Nanostructured Thin Films Materials**

Currently, many of the technologies concentrate on minimizing the materials into nanometric sized materials with nanothickness that leads to the rise of new and exclusive behaviors of such nanomaterials in electronic applications. Hence, this results in a new branch of materials science known as thin films coating. Thin film is 2D nanostructured materials that can be known as a thin material layers with thickness range from nanometers to micrometers. Thin films nanostructured materials are considered as polycrystalline or amorphous, depending on the conditions of its preparation as well as the nature of the material. Thin films consists of materials layer deposited on substrate which can be composed of several layers arrangement [58,59]. Thin film applications are found to be in photovoltaic cells, electronics, sensors, radiation detectors, anti-reflection coatings, reflection, solar energy conversion etc. The developments of new materials with exotic properties of the thin film characterization techniques will certainly attract great attention in future technology.

## **2.5 Method of Nanostructured Layer Deposition**

There are two basic deposition techniques for nanostructured layer employed. The techniques are physical and chemical depositions;

### **2.5.1 Physical Deposition Techniques**

Physical deposition techniques are techniques that depend on thermodynamic and/or mechanical methods to synthesize thin film without any involvement of chemical reactions. They are generally operated in environments of very low pressure in getting efficient results. The deposition involves a physical process of

material transformation from a condensed matter phase to vapor phase and then reformed again to condensed state as thin film. The most commonly known physical deposition processes are sputtering (DC and RF) and evaporation (thermal, arc, electron beam and laser beam).

### 2.5.1(a) Sputtering technique

Sputtering techniques are commonly utilized for metal and oxide thin films deposition for which the morphology, thin film thickness and surface roughness are controlled. A simple system of the sputtering machines comprises an evacuated chamber enclosing a metallic cathode and anode that operate with an applied voltage of several volts and pressure of about 0.01 mbar above. The mechanism of sputtering process depends on ions bombardments that were produced from the discharge to the cathode molecules resulting to molecules liberation from the cathode with a very high kinetic energy. To obtain the maximum momentum transfer; the atomic weight of the bombarding ions must be like the material target. These molecules strike on the anode on straight lines and form a dense thin film layer on the substrate [60-62]. The sketch of the system for sputtering is shown in diagram of Figure 2.2.

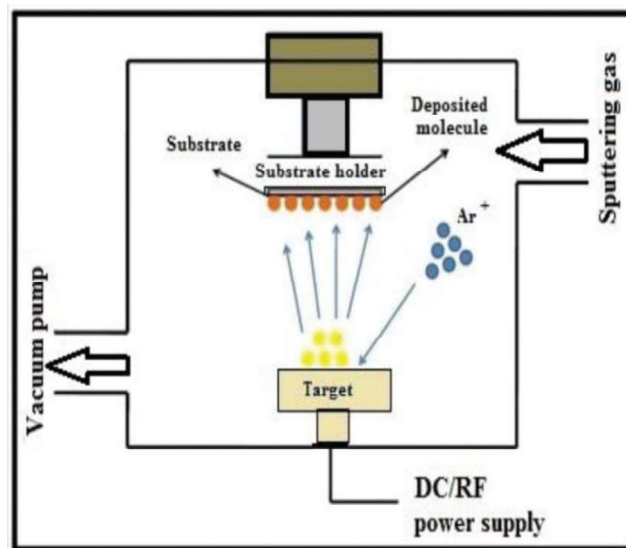


Figure 2.2: Simple sketch of sputtering system [61].

The sputtering technique uses high vacuum applications which result in obtaining a highly purified thin film with great quality. The reactive gases that are compatible for used with sputtering sources are argon, oxygen or nitrogen. The two commonly used sputtering processes are radio frequency (RF) sputtering (metal and metal oxide deposition) and direct current (DC) sputtering (for only metal deposition). The first one depends on RF power while second depend on DC power, which uses an electrically conductive materials target [62].

### **2.5.2 Chemical Deposition Techniques**

Though the thin films formation using physical methods gives good uniformity with great quality and functionalizes properties but appears to be expensive. Subsequently, there is higher demand of good-quality thin films production that is economical low cost. Hence chemical deposition techniques are techniques that are cheaper in producing high thin films with inexpensive equipment that made it to be applied widely. The deposition depends on the pH value, solutions composition, viscosity, concentration etc. The most widely used chemical deposition techniques are chemical bath deposition, sol gel, electrochemical deposition, spray pyrolysis technique and chemical vapor deposition. This section concentrates only on chemical bath deposition techniques been considered as a cheaper technique that forms good quality thin film [61,63].

#### **2.5.2(b) Chemical bath deposition technique**

Chemical bath deposition method is a solution-based technique for thin film growth. It is the oldest solution-based deposition method of thin films. The technique is mostly used to synthesize metal oxide thin film on substrate. The precursor solution of metal ions for solution growth method must form complex solution by the

added capping agents and controlling the solution pH value. Substrates are immersed at a specific desired position within the solution at an angle, horizontal or vertical position under a desired temperature range of 25 – 100 °C and then left it inside the solution to a certain time, till the preferred thin film thickness is achieved. The hydroxide film can then be transformed into the required metal oxide by thermal annealing process at temperature range of 100 - 700 °C [64]. Figure 2.3 shows the simple setup of chemical bath deposition method.

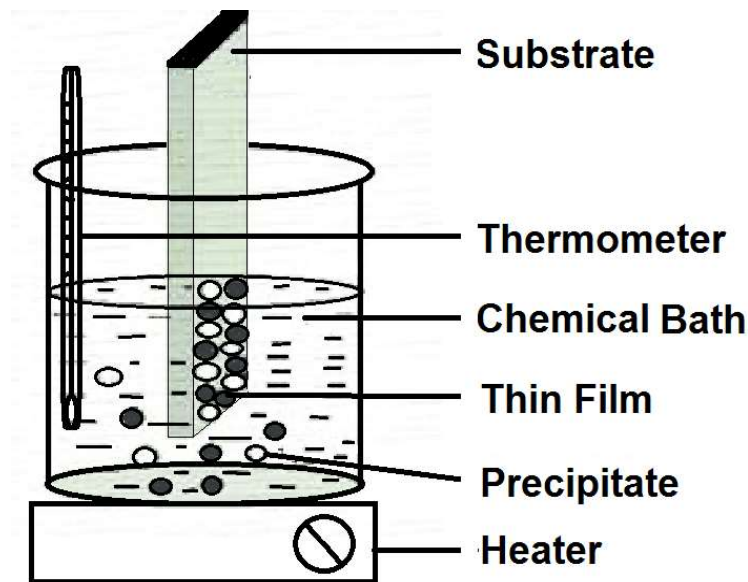


Figure 2.3: Simple setup for chemical bath deposition (modified from [65])

## 2.6 Substrate Materials for Film Deposition

The selection and cleaning procedures of substrate is important in thin film properties. Good quality thin films that have been characterized with special properties are also achieved by following decent steps for substrate cleanliness. The film adhesion and growth highly depend on the substrate influence due to its nature of the surface and the bulk properties. The most commonly used substrate for thin films materials are ceramic, alkali halides, glass, mica, quartz metals, plastics, organic materials and semiconductors material, such as crystalline silicon or germanium, etc. [66]. These substrates are usually applied for epitaxial growth. The well adherent of thin film to

the substrates is the most important for deposition layer. The substrates are selected based on the thin film properties and applications. Lack of appropriate substrate used for preferred deposition results in several experimental restrictions. The properties of the substrate types, structure, rigidity or flexibility, thermal expansion, dielectric strength, electrical or thermal conductivity, melting point and transmittance are noted before general selection of substrate in deposition of thin film [67].

## 2.7 Nickel Oxide

The discovery of nickel metal from its mineral “niccolite” was made by Sweden person known as Axel Fredrik Cronstedt in 1751. Nickel is a metal with colour of silvery white polish. It is malleable, ductile, hard and partially electrical and heat conductor. Nickel is characterized by cubic crystal structure [68,69].

Nickel oxide belongs to transition metal oxide which are generally characterized as materials with variable composition phases. This is because of its non-stoichiometry nature. The sensitivity of surfaces of the transition metal oxide to conditions of preparation are more than that of oxides of non-transition metal. The classification type of transparent metal oxide is based on deficiency of the ion type. For n-type its deficiency is on anion (oxygen deficient), while for p-type (such as the NiO) its deficiency is on cation (nickel deficient or oxygen surplus). The nickel oxides exist in two forms this include; Ni<sub>2</sub>O<sub>3</sub> (Nickel (III) Oxide) and NiO (Nickel (II) Oxide), but the NiO is the most stable [70]. Nickel oxide is commonly known to have cubic crystal structure with lattice parameters of 0.41769 nm [71]. The NiO structure is somewhat been affected at ordinary temperatures from the NaCl cubic structure, the effect smoothly decreases above room temperature, and above 523 K it reaches the rock salt cubic structure with a lattice angle of exactly 60°. NiO possess six fold coordination of octahedral such as the structure of the rock salt [72]. The two

forms at which NiO mainly exists are the green and black colour texture. The stoichiometric composition nature of exactly one Ni to one O atom exist as the green crystal ( $O_1:Ni_1$ ). While the non-stoichiometric compounds exist as the black crystal material with excess of O and deficient of Ni ( $O_1:Ni_{0.98}$ ). The pure NiO of stoichiometric materials are unstable insulator. Non-Stoichiometric is because of the vacancies of nickel presence which is considered as semiconductor. The unit cell of NiO structure is seen in Figure 2.4 [73,74].

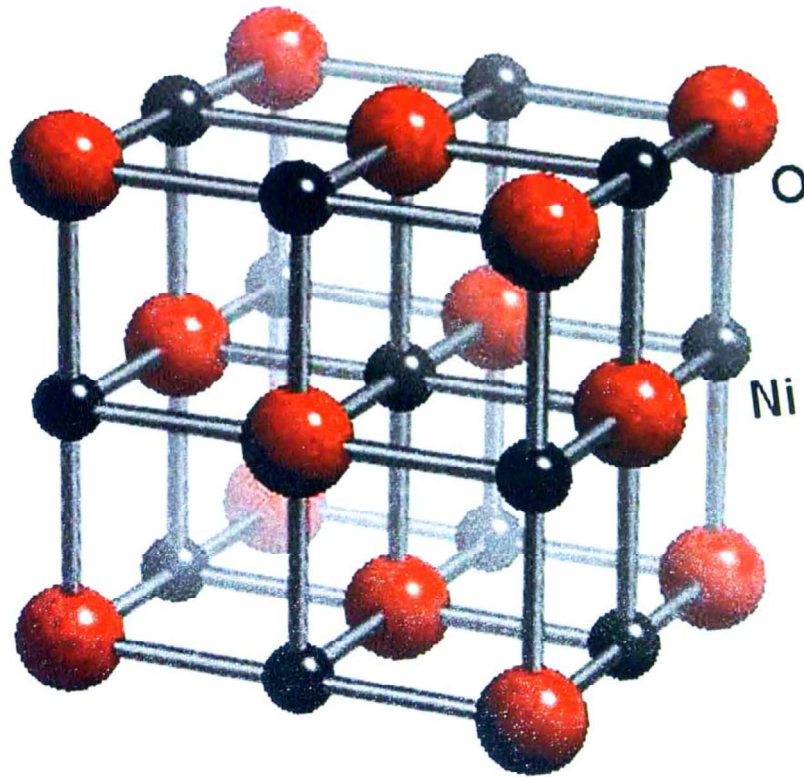


Figure 2.4: Unit cell of NiO [74]

The electronic conductivity in NiO of undoped material is basically because of surplus of oxygen or vacancies of nickel presence. The orientation of NiO ionic crystal thin film is affected mostly by the oxygen ion ( $O^{2-}$ ) arrangement, if the active oxygen and nickel species impinge distinctly on the thin film surface growth. This is because NiO has no direct combination between  $O^{2-}$  and  $Ni^{2+}$  and the  $Ni^{2+}$  ion radius (0.069 nm) is small than that of  $O^{2-}$  ion radius (0.140 nm) [75]. The large size of

oxygen atom makes it difficult to be in the interstitial site of NiO crystal structure. As such this result in the vacancies creation that will usually occupied Ni sites due to excess of oxygen atom in NiO which are seen in Figure 2.5. For complete electrical neutrality preservation in the crystal, two  $\text{Ni}^{2+}$  ions must be transformed to form  $\text{Ni}^{3+}$  ions for each  $\text{Ni}^{2+}$  site vacancy. The jumping of the electron from site of  $\text{Ni}^{2+}$  to  $\text{Ni}^{3+}$  site, is like the movement of positive hole through the sites of  $\text{Ni}^{2+}$ . Hence excess of oxygen in NiO atom is considered as p-type semiconductor. The doping of lithium into NiO increased its conductivity [76]. The radius of crystal Li ions (0.06 nm) is like that of  $\text{Ni}^{2+}$  ion radius (0.069 nm). Thus, this makes Li ion to replace  $\text{Ni}^{2+}$  easily with no significant structural distortion. For electrical neutrality maintenance, one  $\text{Ni}^{2+}$  ion is oxidized the gaining electron to  $\text{Ni}^{3+}$  ion for each Li that is introduced into the structure [77]. Table 2.1 summarized the fundamental properties of NiO.

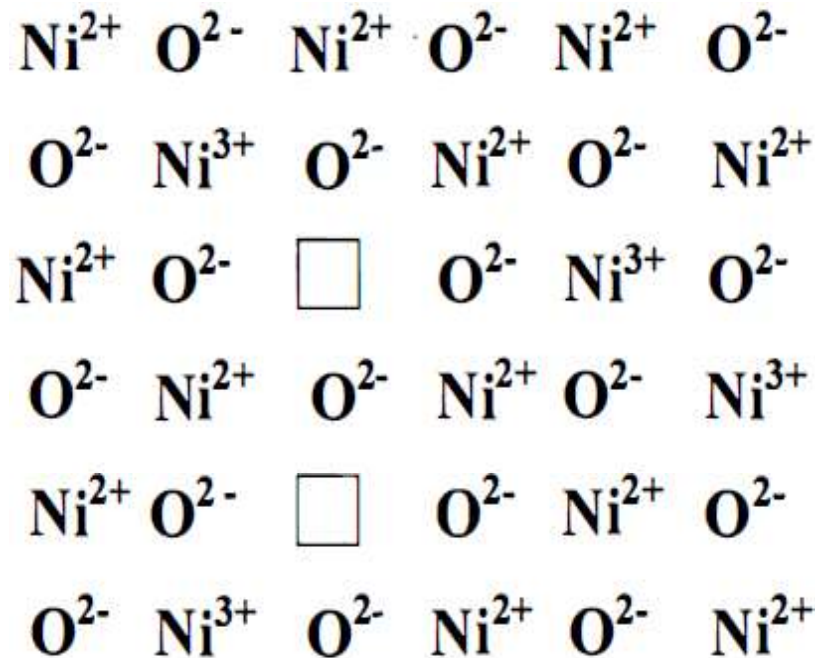


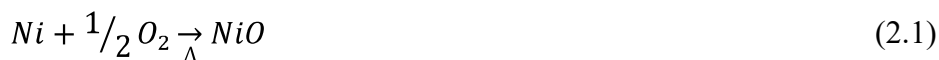
Figure 2.5: Excess "O" in NiO leads to cation vacancies and makes it a p-type semiconductor [74]

Table 2.1 Fundamental properties of NiO

Chemical Symbols	NiO [78]
Chemical Composition	Nickel = 78.55 % and Oxygen = 21.40 % [78]
Appearance	Stoichiometric (O <sub>1</sub> :Ni <sub>1</sub> ) = green (unstable) and Non-stoichiometric NiO (O <sub>1</sub> Ni <sub>0.98</sub> ) = black (stable) [73,74]
Molar Mass	74.6928 g/mol [78]
Melting point	1955 °C [78]
Density	6.67 g/cm <sup>3</sup> [78]
Solubility in water	1.1 mg/L [78]
Magnetic susceptibility	+660.0×10 <sup>-6</sup> cm <sup>3</sup> /mol [78]
Refractive index	2.1818 [78]
Energy band gap	~ 4.0 eV [3]
Lattice constant	0.41769 nm [71]

## 2.8 Thermal Oxidation of Nickel

Thermal oxidation can be defined as the method of oxide layer formation on a material surface. It involves diffusion or reaction of an oxidizing agent (oxidant) forcefully into the material at very high temperature. The applications of thermal oxidations are seen on several materials especially metal. But the main concern is on the oxidation of nickel metal thin film to form the required NiO. The dry oxidation process occurs under clean atmospheric oxygen. The nickel and oxygen react to form nickel oxide under high annealing temperature. The oxidation rate is used to accurately control the oxide thickness [79].



## 2.9 Oxidation Mechanism of Nickel

When an oxygen molecule is in contact with the surface of nickel metal, dissociation into atoms occurs as result of chemisorption that creates bonds of Ni-O on the surface with the nickel underlying below. This reaction is considered as

spontaneous, because within short time the surface layer will be covered entirely with bonded atoms. With the wide covering of the thin film surface, tiny oxide crystals nucleation occurs. As the nuclei are made, they speedily grow and cover the surface of metal with a coherent layer of the oxide. The growth of oxide occurs slowly and continually, which grows into oxide layer by diffusion process of the reactants. Electrons migrate (to neutralize the oxide system) into the oxide layer from the metal and the adsorbed oxygen atoms react with electrons to produce oxide ions. This result in creation of vacancies on the surface at the sites of Ni and the new vacant sites are then occupied by Ni ions. In this case two interfaces are involved; the overall result is like vacancies flow from the interface of nickel oxide-oxygen molecule ( $\text{NiO-O}_2$ ) at surface then inner to the interface of Nickel-Nickel oxide ( $\text{Ni-NiO}$ ); where the annihilation of the vacancies occurs by fusion with Nickel ions from the metal. The liberated electrons at this point move over to the layer of oxide then outward to the surface, where more oxygen atoms are reduced [73].

## **2.10 Synthesis of Nanostructured NiO Materials**

Several methods were employed in synthesizing Nickel oxide thin film with high quality that can be of great use for fundamental applications in electronic device. In this work two different methods were utilized in producing nanostructured NiO layer which involved the physical and chemical method deposition. Therefore, the physical method used, is the thermal oxidation of Ni metal thin film deposited using RF sputtering and the chemical method used, is the chemical bath deposition of nickel hydroxide deposition. Based on these methods, some related literatures reports were considered for comparison with the present project.

### **2.10.1 Reviews on synthesis of Nanostructured NiO layer by Thermal Oxidations of Nickel Metal Thin Film**

Many researchers have work on the synthesis of NiO pertaining to thermal oxidation of nickel nanomaterials. Noh *et al.* (2006), deposited Ni thin films for micro-flow sensors application by RF sputtering and oxidized under annealing temperature range of 300 - 500 °C for 5 h. The oxidation extent of Ni thin films was observed to be directly on the annealing temperatures function. They assumed that the rate of oxidation may also directly depend on the annealing time. Likewise from the XRD analysis Ni peak appears to increase at lower (500 below) temperature with weaker peak of NiO, But at higher temperature (500 °C above), Ni peak become lower with increasing of NiO peak intensity that shows high crystal quality of NiO at higher annealing temperature [80]. Courtade *et al.* (2008), synthesis NiO from thermal oxidation of metallic Ni thin film with thickness of 100 nm at room temperature on silicon substrates using 2000 W DC power source. Different parameters were used for thin film optimization which are the oxidation time (10 - 1800 s), partial pressure of oxygen (20 and 500 ppm) and temperature (200, 300 and 400°C) [81]. In (2008), Zhang et al., produces 2D NiO nanowalls by thermal oxidation of a Ni thin film deposited on stainless steel substrate by sputtering. The oxidation duration time shown a significant effect on the Ni thin film conversion to NiO nanowalls with optimum annealing temperature at 600 °C for 4 hours [82]. Mohanty *et al.* (2010), synthesized NiO film by thermal oxidation at 500 °C of nickel thin film (200 nm thickness) deposited by thermal evaporation on ITO/glass substrate for different annealing time of 3 - 6 hours. They interpret the sandwiched of nickel layer existing between ITO and NiO layer which indicate incomplete oxidation, suggesting that complete oxidation can be achieved with thinner film of Ni film. The

mechanism of NiO growth was based on nickel atoms diffusion from nickel layer film which may likely required high activation energy [83]. The grown NiO nanocrystalline thin film were successfully made on glass substrates by Venter and Botha (2011), using thermal oxidation (350 - 600 °C) of 1000-Å thick Ni layers, with the optimal oxidation temperature of 450 °C for a period of 2 ½ hours. Cubic NiO crystal with (111) and (200) reflections was confirmed from the XRD results with the oxidation temperature of 400 °C and above [84]. Koga and Hirasawa (2013), synthesize NiO nanorods with great crystal quality using rapid thermal oxidation of Ni nanoparticles treated under 400 °C [85]. P-type NiO-based TFTs (thin film transistor) was fabricated on silicon wafer by Jiang et al., (2013) using thermal oxidization of Ni films with 30 nm thicknesses. Annealing at 400 °C for 1 hour was observed to have an incomplete oxidation with oxide layer at the thin film upper part while the bottom maintained to be as the as grown metallic Ni metal thin film [86]. Saleh (2013), grown NiO from thermal evaporation at 850 °C of Ni film in a vacuum system with high purity. The nickel film was deposited on quartz substrate under low pressure at RT with thickness of 150 nm. The condition of oxidation used in optimization of NiO film formation was different oxidation time of 30 and 60 sec, with the higher crystal quality at 60 sec grown film. The crystal size of prepared NiO films obtained was in 49 to 63 nm range [1]. The thermal oxidation of nickel thin films (50 nm thickness on polished Si/SiO<sub>2</sub> substrates using conventional thermal evaporation) was also confirmed by Luis *et al.* (2014). The granular formation of NiO depends on annealing temperature which as well promotes the thin films growth. The annealing was performed under the temperature of 300, 325, 350, 400, and 700 °C. An incomplete oxidation of the film was observed at 400 °C below, while a complete oxidation was obtained at higher temperature of 700 °C [87].

Table 2.2 The survey of NiO synthesized from literature by thermal dry oxidation of Nickel

Subs.	Ni Deposition				Thermal Oxidation (NiO Growth)		2 $\theta$ XRD peak ( $^{\circ}$ )	Morphology	Bandgap (eV)	Ref.
	Method	Power (W)	Temp. ( $^{\circ}$ C)	t (nm)	Temp. ( $^{\circ}$ C)	Duration (hr)				
-	laser ablation	-	900	-	400	-	-	nanorods	-	[85]
stainless steel	Sputtering	-	50	1000	600	4	43	nanowall	-	[82]
SiO <sub>2</sub> /Si	Electron-beam evaporator	-	-	30	400	1	43	nanocrystal	3.70	[86]
Glass	thermal evaporation	-	RT	100	450	2.5	37	nanocrystal	3.76	[84]
Al <sub>2</sub> O <sub>3</sub>	R.F. sputtering	7	RT	-	400	5	43	-	-	[80]
SiO <sub>2</sub> /Si <sub>3</sub> N <sub>4</sub> /Si	dc physical vapor deposition	2000	RT	100	400	0.5	37	-	-	[81]
Si/SiO <sub>2</sub>	thermal evaporation	-	RT	50	700	3	37	-	-	[87]
ITO/Glass	thermal evaporation	-	RT	200	500	6	37	-	3.80	[83]
quartz	thermal evaporation	-	RT	150	850	0.1	37	nanosize	-	[1]

Table 2.2 have shown different reports for thermal oxidation of Ni thin film. The substrate, deposition method, operating power, temperature and film thickness of Ni thin film plays a great role in obtaining different result of NiO properties with layer enhancement after the thermal oxidation. Therefore, these parameters were considered and varied for the growth of NiO layer for better result of H<sub>2</sub> gas sensor.

### **2.10.2 Reviews on synthesis of Nanostructured NiO layer by Chemical Bath Deposition**

In review of chemical bath deposition, several researches have been conducted with this method. But different NiO layer properties was obtained due to different solution mixture and deposition condition. Igwe *et al.* (2009) obtained NiO thin films by CBD technique on glass substrates using hydrated nickel sulphate (NiSO<sub>4</sub>•6H<sub>2</sub>O of 1 M), potassium chloride (KCl of 1 M), and complex agent of Ammonia (NH<sub>3</sub> of 1 M) in a beaker of 50 ml. The solution after immersing the substrate inside undergoes thermal treatment in the oven for about 75 °C for 3 hours with film thickness range of 0.12 - 0.14 μm. The as-grown Ni(OH)<sub>2</sub> thin film undergo thermal treatment to NiO films after exposed to post-deposition annealing at different temperatures of 100, 150, 200, 300 and 399 °C [88]. Mendoza-Galván *et al.* (2009) synthesis NiO thin films were prepared using CBD with precursor mixture of Ni(NO<sub>3</sub>)<sub>2</sub> (0.06 M) and urea (12.6 g) resulting in 84 ml volume of the total bath. After immersing the ITO/glass substrates vertically with the bath container walls support and treated at temperature of 90 °C for 30 min, Ni(OH)<sub>2</sub> thin films were obtained with a porous nanostructure of wider surface area and thickness of 420 nm. Ni(OH)<sub>2</sub> was transformed to NiO by annealing at 200 - 600 °C for 30 min with the optimum growth temperature at 300 °C [71]. In 2010, Xiao *et al.* synthesized NiO by CBD using nickel sulfate (1 M), potassium persulfate (0.25 M) and aqueous

ammonia (1 M). The obtained hierarchically porous-structured thin film with 30–250 nm pores diameter was annealed at 350 °C for 90 min [89]. The report made by Xia et al. (2011) shows the synthesis of hierarchically porous NiO film obtained by combining a CBD method with polystyrene (PS) sphere template using nickel foil substrate. The CBD mixture solution consist nickel sulfate (1 M), potassium persulfate (0.25 M) and aqueous ammonia (1 M). The substrate was vertically placed into the solution for 30 min to obtain the required film deposition at room temperature. Then, finally the required NiO film was obtained by annealed for 90 min at 350 °C [90]. Dalavi (2012), have grown NiO thin films by CBD with solution precursor of nickel sulfate and potassium chloride and aqueous ammonia with ITO/glass substrate. The substrates were vertically placed into the prepared solution at RT with subsequent removal of the substrate at different interval time of 10, 20, 30, 40, 50 and 60 min. The deposited films were then annealed for 90 min at 300 °C. This result is obtained with different thin film thickness with the optimal parameter at 60 min [91]. Offiah *et al.* (2014), synthesized NiO layer on glass substrates by CBD with a solution mixture of NiSO<sub>4</sub> (2 ml of 1 M), KCl (12 ml of 1 M) and NH<sub>4</sub>OH solution (35 ml of 1 M). 90 ml of the total volume was achieved with PVP solution addition of 40 ml into a beaker of 100 ml. The deposit process occurs at RT for a period of 420 min. Another 180 min was added to increase the film thickness. The films were annealed at different temperature of as-grown film at 100, 200, 300 and 400 °C. Optical band gap decreased with the different decomposition temperatures from 2.7 to 2.2 eV [92].